Published in final edited form as:
Exp Hematol. 2012 December ; 40(12): 1016–1027. doi:10.1016/j.exphem.2012.08.001.

Gene expression profiling and candidate gene re-sequencing identifies pathways and mutations important for malignant transformation caused by leukemogenic fusion genes

Rachel L. Novak[1], **David P. Harper**[2], **David Caudell**[1], **Christopher Slape**[1], **Sarah H. Beachy**[1], and **Peter D. Aplan**[1]

[1]Leukemia Biology Section, Genetics Branch, Center for Cancer Research, National Cancer Institute, National Institute of Health, Bethesda, MD

[2]Department of Pediatrics, Uniformed Services University of the Health Sciences, Bethesda, MD

Abstract

NUP98-HOXD13 (*NHD13*) and *CALM-AF10* (*CA10*) are oncogenic fusion proteins produced by recurrent chromosomal translocations in patients with acute myeloid leukemia (AML). Transgenic mice that express these fusions develop AML with a long latency and incomplete penetrance, suggesting that collaborating genetic events are required for leukemic transformation. We employed genetic techniques to identify both pre-leukemic abnormalities in healthy transgenic mice as well as collaborating events leading to leukemic transformation. Candidate gene resequencing revealed that 6 out of 27 (22%) *CA10* AMLs spontaneously acquired a *Ras* pathway mutation and 8 out of 27 (30%) acquired a *Flt3* mutation. Two *CA10* AMLs acquired a *Flt3* internal-tandem duplication, demonstrating that these mutations can be acquired in murine as well as human AML. Gene expression profiles revealed a marked upregulation of *Hox* genes, particularly *Hoxa5*, *Hoxa9*, and *Hoxa10* in both *NHD13* and *CA10* mice. Furthermore, mir196b, which is embedded within the *Hoxa* locus, was overexpressed in both *CA10* and *NHD13* samples. In contrast, the Hox cofactors *Meis1* and *Pbx3* were differentially expressed; *Meis1* was increased in *CA10* AMLs but not *NHD13* AMLs, whereas *Pbx3* was consistently increased in *NHD13* but not *CA10* AMLs. Silencing of *Pbx3* in *NHD13* cells led to decreased proliferation, increased apoptosis, and decreased colony formation *in vitro*, suggesting a previously unexpected role for *Pbx3* in leukemic transformation.

Keywords

CALM; *AF10*; *NUP98*; *HOXD13*; *Hoxa9*; *Meis1*; *Pbx3*; acute myeloid leukemia (AML)

Correspondence to: Peter D. Aplan, Genetics Branch, Center for Cancer Research, National Cancer Institute, National Institutes of Health, 41 Center Drive, Bethesda, MD 20892, USA, PH: 301-435-5005, FAX: 301-496-0047, aplanp@mail.nih.gov.

Conflict of Interest Disclosure:
P.D.A. and C.S. have received royalties from the NIH Division of Technology Transfer for the invention of NUP98-HOXD13 mice.

Introduction

Recurrent, balanced chromosomal translocations have been identified in a wide range of hematologic malignancies [1]. These translocations typically produce aberrant fusion proteins, the study of which has been a rich source of insight into leukemic transformation [2, 3]. Oncogenic fusion proteins resulting from balanced chromosomal translocations involving *MLL*, *NUP98*, or *CALM* produce aberrant transcription factors; whose expression typically leads to upregulation of *Hoxa* cluster genes and their co-factors, such as *Meis1* [3–5]. Overexpression of *Hoxa9* and *Meis1* has been identified in approximately half of all patients with acute myeloid leukemia (AML) [6–11], with *Hoxa9* overexpression as a marker for poor prognosis AML [6]. Several mouse models of AML have further highlighted the importance of *Hoxa9* and *Meis1* in leukemic transformation [12–15].

Expression of the oncogenic fusion proteins *NUP98-HOXD13 (NHD13)* or *CALM-AF10 (CA10)* in the hematopoietic compartment of mice results in the development of AML, with a long latency and incomplete penetrance [16, 17]. The AMLs that develop in these mouse models have an aggressive nature and features of B cell differentiation, including expression of the B-cell antigen B220 and clonal *Igh* gene rearrangements [16–18]. The *NHD13* and *CA10* leukemias share these features, as well as the overexpression of *Hoxa9*, with AML induced by *MLL*-fusions [3, 11, 14]. The late onset of leukemia in the *NHD13* and *CA10* murine models strongly suggests that expression of the oncogenic fusion proteins is required, but not sufficient, to promote leukemogenesis [16, 17]. This observation is consistent with the hypothesis that leukemic transformation requires complementary mutations that affect at least two different conserved pathways in hematopoietic stem/progenitor cells: one impairing maturation or self-renewal and the second promoting aberrant proliferation [19].

In this study we employed candidate gene resequencing and gene expression arrays (GEAs) to compare and contrast the biological pathways that are dysregulated in *CA10* and *NHD13* mice. We analyzed gene expression profiles (GEPs) from clinically healthy *CA10* and *NHD13* tissues to establish the direct effect of these transgenes on global gene expression in hematopoietic tissues. Subsequent analysis of GEPs from both clinically healthy and leukemic tissues highlighted important similarities and differences between the *NHD13* and *CA10* models including a similar deregulation of *Hoxa* cluster (*Hoxa5*, *Hoxa9*, and *Hoxa10*) genes and striking differences in expression of the *Hoxc* cluster genes and the TALE homeodomain proteins *Meis1* and *Pbx3*.

Materials and Methods

Leukemia Diagnosis

Generation of *CA10* and *NHD13* mice and leukemia diagnosis has been described previously [16, 17]. Leukemia diagnoses were made according to the Bethesda proposals [20, 21]. Tissues obtained from *CA10* or *NHD13* mice in which no gross signs of leukemia were evident were described as clinically healthy.

Targeted Gene Resequencing and PCR analysis of *Flt3* Length Mutations

Genomic DNA was amplified with the primer sets listed in Supplemental Table 1. PCR products were gel purified (Qiagen) and sequenced by the Sanger method. To confirm *Flt3* length mutations, PCR products were sub-cloned into the pGemT-Easy Vector (Promega) and sequenced as above. Analysis for loss of the WT *Flt3* allele in *CA10* mice harboring an *Flt3* length mutation was done by PCR analysis using primers flanking the region of the length mutations (Supplemental Table 1).

Isolation of Lineage Negative Bone Marrow (LNBM)

LNBM was isolated by negative selection using EasySep Mouse Hematopoietic Stem Cell enrichment kit (Stem Cell Technologies) according to the manufacturer's protocol. LNBM was cultured in Iscove modified Dulbecco medium (IMDM) (Invitrogen) supplemented with 15% FBS, 100mM L-Glutamine and 10μg/ml Penicillin/Streptomycin (Invitrogen), 50ng/ml recombinant mouse Stem Cell Factor (SCF), 10ng/ml recombinant mouse interleukin 3 (Il3), and 10ng/ml recombinant human interleukin 6 (IL6) (R&D Systems) at 37°C at 5% CO_2.

RNA isolation, cDNA synthesis and reverse transcriptase quantitative polymerase chain reaction (RQ-PCR)

RNA was isolated using Trizol (Invitrogen) reagent and the manufacturer's protocol. 1μg of RNA was used to synthesize cDNA with Superscript III Reverse Transcriptase (Invitrogen) in a 20 uL reaction according to the manufacturer's protocol. For RQ-PCR analysis, 1 μl of cDNA was amplified using Taqman primer and probe sets (Applied Biosystems) as indicated in figures or Supplemental Table 1. RQ-PCR analysis was performed on a 7500 Fast RT-PCR system (Applied Biosystems) using the default thermal cycling conditions. 18S ribosomal RNA was used as an internal control. ΔCT values were -log2 transformed and normalized to wild type (WT) bone marrow (BM).

GEAs and Gene Set Enrichment (GSEA)

RNA samples were hybridized to Affymetrix Mouse 430 2.0 arrays (Laboratory of Molecular Technology, Frederick, Maryland, USA). Gene expression data was analyzed using BRB Array Tools (see Acknowledgments). To generate tables of differentially expressed genes, genes with a 1.5 fold difference in expression and a parametric p-value less than 0.05 were tabulated. Probe sets with log2 transformed geometric mean intensities below 100 were not included in the analysis. For the analysis of leukemia samples, obtained from infiltrated spleens, genes increased 5.0 fold in normal spleens compared to normal BM were filtered out. For GSEA analysis, tissue comparisons listed in the figures were analyzed using the GSEA software [22, 23] and compared to AML gene signatures were taken from the Broad database. Leading Edge Analysis was performed comparing gene lists generated from *CA10* AMLs/WT LNBM comparisons to previously described *MLL*-associated gene lists [24, 25].

microRNA Expression

10ng of RNA was reverse transcribed using the miRNA reverse-transcription kit and primer set for mir196b (Applied Biosystems) according to the manufacturer's protocol. 1.3μl of cDNA was used for RT-PCR analysis under the following cycling conditions: 95°C for 10 minutes, 95°C for 15 seconds, and 60°C for 1 minute for 40 cycles. The U6 primer/probe set was used as an internal control. ΔCT values were -log2 transformed and normalized to WT BM.

Lentiviral Infection

pLKO.1-puro constructs containing three different short hairpin RNA (shRNA) inserts against either murine *Pbx3* (sh*Pbx3*-1, sh*Pbx3*-2, sh*Pbx3*-3) or a scrambled non-targeting (NT) control (Sigma Aldrich) were co-transfected with pVSV-G and pΔR8.2 into the 293T cell line using calcium phosphate. 48 hours post-transfection, viral supernatants were used to infect 189MIG cells, a green fluorescent protein-tagged derivative of the Il3-dependent 189L2 cells that express the NHD13 protein [26]. 189MIG cells were incubated in 4mls of unconcentrated viral supernatants in the presence of 10ng/ml Il3 and 100μg/ml protamine sulfate for 24 hours at 37°C. Cells were washed and incubated for an additional 24 hours in complete media supplemented with Il3 before the addition of 1μg/ml of puromycin. To

generate single cell clones of infected cells, cells were plated in a 96-well plate at 0.7 cells/well and grown in the presence of Il3 and puromycin for 10 days.

Cell Proliferation, Apoptosis and Methylcellulose Assays

Uninfected 189MIG cells or cells infected with shRNA particles were plated at a density of 5.0×10^4 in a 12-well dish and incubated in complete IMDM media supplemented with Il3. Viable cell number was determined by trypan blue exclusion. For methylcellulose cultures, uninfected or shRNA-infected 189MIG cells were plated at a density of 1×10^3 in M3434_methylcellulose (Stem Cell Technologies) and incubated at 37°C for 10–14 days. For cell cycle assays, cells were washed, fixed/permeablilized and incubated at 4°C for 30 minutes. Cells were washed and resuspended in PBS supplemented with 180 μg/ml propidium iodide and 15 μg/ml RNase for 30 minutes at room temperature and analyzed by flow cytometry for DNA content.

Results

Candidate gene resequencing identifies mutations in *CA10* AMLs

We sequenced portions of *Nras*, *Kras*, *Ptpn11*, *Flt3*, *Kit*, *Idh1*, *Idh2*, and *Wt1* from 27 *CA10* leukemic spleens (Table 1 and Supplemental Table 2). No mutations were identified in *Kit*, *Idh1*, *Idh2* or *Wt1* (Supplemental Table 2), however, 3 of the 27 (11%) had acquired an *Nras* mutation and 2 of 27 (7%) acquired a *Kras* mutation in codons 12, 13, or 61. Activating mutations of *Ptpn11,* a downstream effector of Ras signaling, have been identified in patients with juvenile myelomonocytic leukemia (JMML), myelodysplastic syndrome (MDS), and AML [27]. We sequenced exons 3 and 13 of *Ptpn11,* corresponding to the regions most frequently mutated in leukemic patients, and identified one activating mutation in exon 3 of *Ptpn11*. In sum, 6 of 27 (22%) *CA10* leukemic samples had acquired activating mutations of the Ras pathway; this frequency was comparable to that previously reported for *NHD13* leukemias (32%) [28].

Flt3 is a receptor tyrosine kinase frequently mutated in AML patients; these mutations most commonly take the form of single nucleotide substitutions within the tyrosine kinase domain (TKD) or internal tandem duplications (ITDs) within the juxtamembrane domain (JM) [29]. We analyzed *CA10* leukemias for ITD mutations in exons 14–15 or for TKD mutations in exon 19, and identified acquired mutations in 8 of 27 (30%) *CA10* samples (Table 1). Six mice had acquired TKD mutations; four had an identical GAC>GCC transversion at codon 841, resulting in a D>G change, one had a GTC>GCC transition at codon 822, resulting in a V>A change, and one had an in frame deletion of codon 837, which encodes aspartic acid. Although mutations similar to the D>G missense substitution and the D deletion have been reported in AML patients [30, 31], the V>A substitution has not been reported and it is unclear whether this V>A substitution is oncogenic. Of note, this mouse also has an oncogenic *Kras* mutation (Table 1).

Interestingly, we identified two *CA10* leukemias that harbored *Flt3*-ITD mutations in the JM domain. These samples had 12 or 39 bp in-frame insertion which occurred at the identical nucleotide within exons 14 of *Flt3* (nucleotide 1778, codon 593 of NM_010229 coding sequence) (Figure 1). Since some AML patients with *Flt3*-ITD mutations lose the remaining WT *Flt3* allele [29–31] and the sequence electropherograms of the PCR products did not show two overlying tracings, we hypothesized that the wild-type allele had been lost. To test this, we amplified the region containing the *Flt3* length mutations. PCR analysis showed only the mutant allele, with no evidence for retention of the WT allele, consistent with the electropherogram tracing (Figure 1C). In contrast to the *Flt3*-ITD mutations, loss of the WT allele in AML patients with an *Flt3*-TKD mutation is a rare event, reported in approximately

4% [30, 31]. Consistent with that observation, analysis of sequence tracings from *CA10* leukemias with *Flt3*-TKD mutations did not show loss of the WT allele (Figure 1D).

To determine if *Flt3* expression was increased in the *CA10* mice with a *Flt3* mutation, we performed RQ-PCR assays. *Flt3* expression was modestly increased in BM from clinically healthy *CA10* mice compared to WT mice, but was significantly up-regulated (18.0 fold) in *CA10* AML samples (Figure 1E). In contrast, there was no difference in expression of *Flt3* in AML samples or BM from clinically healthy *NHD13* mice compared to WT BM (Figure 1E). This is consistent with our prior study which showed that none of the 22 AML sample from *NHD13* mice had acquired *Flt3* mutations [28], therefore we concluded that overexpression or mutation of *Flt3* is not a frequent oncogenic event in the *NHD13* mouse model. However, for the *CA10* mouse model, our data strongly suggests that mutation of *Flt3* is a frequent acquired oncogenic event associated with leukemic transformation *in vivo* (Table 1 and Figure 1A–E). Fisher's Exact analysis of *Flt3* mutations from *CA10* (8/27) and *NHD13* (0/22) AMLs showed a statistically significant difference (p=0.0056).

Hoxa9 and *Meis1* are differentially expressed in hematopoietic tissue from *CA10* mice

To determine the effect of enforced expression of *CA10*, we compared the gene expression profiles (GEP) of hematopoietic tissues (BM, LNBM, spleen, and thymus) from clinically healthy *CA10* mice to WT mice (Supplemental Table 3). We purposely chose hematopoietic tissues from non-leukemic *CA10* mice for this study, since we anticipated that any gene expression changes in leukemic *CA10* mice would reflect a combination of changes caused by the primary mutation (the *CA10* transgene), as well as those caused by additional acquired mutations (such as *Nras, Kras,* or *Flt3*). Analysis of GEP revealed a relatively small number of genes whose expression in *CA10* BM differed from WT BM by more than 1.5 fold (Supplemental Table 3). Remarkably, in this unbiased survey, the top two upregulated genes were *Hoxa9* and *Meis1*, two genes that we had previously suspected to be increased in *CA10* leukemias based on published reports [16, 32]. In addition, we previously showed that T and B lymphocyte maturation are abnormal in *CA10* mice [16]; therefore, we compared the GEP's of *CA10* thymus and spleen to that of WT thymus and spleen (Supplemental Table 3). Similar to findings in BM, *Hoxa* cluster genes (*Hoxa9* and *Hoxa5*) and *Meis1* were among the most highly upregulated genes in the *CA10* thymus and spleen. Finally, to determine the effect of enforced expression of *CA10* on hematopoietic stem/progenitor cells, we compared the GEP of immature cells from *CA10* and WT LNBM (Supplemental Table 3). Again, *Hoxa9*, *Hoxa5*, and *Meis1* were amongst the most significantly increased genes.

To determine a gene signature generally associated with the expression of *CA10*, we analyzed the sets of genes that were increased in *CA10* BM, thymus, and LNBM (Figure 2A). We found that *Hoxa9* and *Meis1* were the only genes consistently upregulated in all *CA10* hematopoietic tissues (Figure 2A) suggesting that their upregulation is an important downstream genetic event in tissues expressing *CA10*.

Murine *CA10* AMLs display gene expression patterns similar to human leukemias expressing *CA10* or *MLL* fusions

To identify a gene signature that is important for malignant transformation of hematopoietic cells that expressed a *CA10* fusion, we compared the GEP of *CA10* leukemia samples to that of WT BM and WT LNBM cells (Supplemental Table 4). The comparison of *CA10* AMLs to WT BM again confirmed the up-regulation of *Hoxa9* and *Meis1* at a 17.7 and 17.2 fold, respectively.

We used Gene Set Enrichment Analysis (GSEA) [22, 23] to determine if the GEPs from *CA10*-induced AMLs were similar to that of patients with AML. We found that the *CA10*

AML gene signature shared a high degree of similarity to gene signatures from AML patients harboring *MLL* fusions [24, 25] (Figure 2B). Leading edge analysis of genes that contribute significantly to the signature revealed that *Hoxa5* and *Hoxa9* were two of the most prominent and significant genes in the signature. Taken together, we conclude that the *CA10* mouse AMLs share disruption of similar biological pathways to those seen in patients with AML caused by *MLL* fusions.

Although patients with *CA10* positive leukemias are most commonly gamma/delta T-cell acute lymphoid leukemia (ALL), these leukemias often display myeloid features, such as CD33 or CD34 expression [33]. Using a publicly available data-set [34], we identified 264 genes that were over-expressed at least 1.5-fold in *CA10* positive T-ALL's compared to *CA10* negative T-ALLs and compared that list to the set of genes that was 1.5-fold increased in the murine *CA10* AMLs compared to WT LNBM. We found 79 genes that were up-regulated in both the human *CA10* positive leukemias and the murine *CA10* AML samples (Supplemental Figure 1A), including *Hoxa5*, *Hoxa9*, *Meis1,* and *Brd4*. Furthermore, comparison of our *CA10* associated upregulated genes to the top 100 genes associated with *CA10* in patient samples identified in Mulaw *et al*. [35], identified 27 genes in commonly upregulated including *Hoxa9*, *Meis1*, and *Flt3* (Supplemental Figure 1B) suggesting that expression of *CA10* in transgenic mice dysregulates pathways similar to those disrupted in human *CA10* leukemias.

Hox genes and *Pbx3* are over-expressed in hematopoietic tissues from *NHD13* mice

We previously showed that mice which express a *NHD13* transgene also upregulate *Hoxa* cluster genes [36]. To expand these findings, we compared the GEP of hematopoietic tissues from *NHD13* mice to WT mice. Similar to findings with the *CA10* mice, *NHD13* tissues demonstrated increased expression of *Hox* genes (Supplemental Table 5). *Hoxa9* (9.9 Fold), *Hoxa5* (6.5 fold), *Hoxc4* (4.8 fold) and *Hoxc6* (3.1 fold) were significantly increased in the *NHD13* BM compared to WT; similar trends were detected in LNBM and thymus. The TALE homeodomain family member *Pbx3* was consistently increased in all *NHD13* clinically healthy tissues (4.9–17.4 fold) compared to their WT counterparts (Supplemental Table 5). Of note, *Meis1,* was not identified as a differentially expressed gene in clinically healthy tissue from *NHD13* mice. Similar to the analysis of *CA10* mice, we identified 5 genes that were significantly increased in all *NHD13* BM, LNBM, and thymus; these genes included *Hoxa9*, *Hoxc6*, *Mab21l2*, *Pbx3*, and *B930068K11Rik* (Figure 2C).

To determine which genes and pathways might be important for *NHD13*-mediated leukemic transformation, we analyzed changes in gene expression in the *NHD13* leukemias as above. There were 3073 differentially expressed genes in the *NHD13* leukemias compared to WT BM (Supplemental Table 6). Similar to the findings with *NHD13* BM from clinically healthy mice, *NHD13* AML samples displayed significantly increased levels of several *Hox* genes (*Hoxa5*, *Hoxa7*, *Hoxa9*, and *Hoxc4*) and *Pbx3*.

To identify genes and pathways that are commonly dysregulated in both *CA10* and *NHD13* leukemias, we identified genes that were differentially expressed in *CA10* and *NHD13* AML compared to WT BM (Figure 2D). We found 8 genes that were significantly up-regulated at least 4 fold in both the *CA10* and *NHD13* AMLs: *Hoxa9*, *Psat1*, *Serpinb6b*, *Rpl23*, *Fzrb*, *Plvap*, and *Itgb1*, and 7 genes down-regulated at least 4 fold in *CA10* and *NHD13* AMLs: *Bpgm*, *AA467197*, *Chi3l1*, *Cxcr2*, *Mmp8*, *Mmp9*, and *Scna*.

Verification of *Hoxa* gene locus overexpression in *CA10* and *NHD13* tissues

To further evaluate the expression levels of the *Hoxa* locus (Figure 3A), and portions of the *Hoxc* cluster, we compared the log2 transformed values from the GEAs for *CA10* (Fig 3B)

and *NHD13* (Fig 3C) to WT BM samples. The *Hoxa* cluster genes consistently upregulated in both the *CA10* and *NHD13* leukemias were *Hoxa5*, *Hoxa9*, and *Hoxa10*, with *Hoxa9* showing the most dramatic increase compared to WT BM (Figure 3B and 3C). Although expression of the *CA10* fusion led to relatively minor (<1.5 fold) changes in the *Hoxc* cluster genes examined, *Hoxc4* was significantly increased in BM (5.3 fold), LNBM (4.1 fold) and AML (15.7 fold) from the *NHD13* mice compared to WT BM (Figure 3C). Expression of *Hoxa5*, *Hoxa7*, *Hoxa9*, *Hoxa10* and *Hoxc4* was confirmed by RQ-PCR analysis for both *CA10* and *NHD13* tissues (Figure 3D).

mir196b is a microRNA (miRNA) situated within the *Hoxa* locus between *Hoxa9* and *Hoxa10* (Fig 3A), and has been shown to be overexpressed in some patients with AML, especially those with *MLL* or *CA10* gene fusions [37–40]. Given its location and the observation that *Hoxa9* and *Hoxa10* are increased in *CA10* and *NHD13* leukemias (Figure 3B–C), we suspected that mir196b expression might also be increased in these tissues. RQ-PCR analysis of *CA10* BM and AML samples demonstrated an increase in mir196b expression of 4–11 fold, whereas *NHD13* BM and AML samples showed a more modest 2–3 fold increase (Figure 3E). Taken together, we conclude that dysregulation of the *Hoxa* locus is a common feature in both *NHD13* and *CA10* mice.

TALE homeodomain family members *Meis1* and *Pbx3* are differentially expressed in *CA10* and *NHD13* tissues

TALE homeodomain family members, including *Meis1*, *Pbx1*, *Pbx2,* and *Pbx3* are transcriptional co-factors important for *Hox* function [41]; of these, *Meis1* is most commonly overexpressed in human and murine AML samples [8, 11, 13, 16, 42]. Log2 transformed expression values from GEAs normalized to WT BM is shown in Figure 4A and 4B. *Meis1* is the only TALE gene markedly (>2 fold) upregulated in the *CA10* samples; this upregulation is seen in *CA10* BM samples from clinically healthy and leukemic mice, suggesting that *Meis1* upregulation may be an early or initiating event in -*CA10*-mediated leukemic transformation. In contrast, although a subset of *NHD13* AML samples had clear upregulation of *Meis1* there was not a consistent increase in *Meis1* in tissues from *NHD13* mice, suggesting that *Meis1* overexpression was not required for *NHD13*-mediated leukemic transformation (Fig 4B and 4C). Interestingly, *Pbx3* was consistently upregulated in *NHD13* hematopoietic tissues (Figure 4B and 4D), and was the only TALE mRNA overexpressed in all *NHD13* samples.

Several studies have suggested that *Flt3* gene expression is regulated, at least in part, by *Hoxa9* and *Meis1* [43, 44]. To determine if there was a correlation between *Meis1* and *Flt3* expression in *CA10* and *NHD13* transgenic mice, we compared *Meis1* and *Flt3* gene expression data, as measured by RQ-PCR, from several different sample sets (Figure 4E). There was a strong correlation between *Meis1* and *Flt3* expression (R^2=0.8764) suggesting that *Meis1* may have a direct role in the regulation of *Flt3* expression. Analysis of a publicly available dataset [34] demonstrated a significant correlation between *FLT3* and *MEIS1* expression in the *CA10* positive leukemias but not in the *CA10* negative leukemias, supporting the assertion that this *CA10* mouse model shares a similar biology to *CA10* leukemias in humans (Supplemental Figure 2).

Knockdown of *Pbx3* in an *NHD13* cell line inhibits proliferation and promotes apoptosis

To determine if *Pbx3* is important for leukemic transformation in the context of the *NHD13* fusion, we utilized 189MIG cells, a non-transformed, Il3-dependent cell line that was generated by *in vitro* differentiation of murine embryonic stem cells that express an *NHD13* fusion [26]. 189MIG cells were infected with lentiviral shRNA particles directed against *Pbx3* or a non-targeting (NT) shRNA control and selected with puromycin. Expression of

each *Pbx3* shRNA inhibited *Pbx3* expression to a variable degree (Figure 5A). Cells infected with sh*Pbx3*-1 or sh*Pbx3*-3 showed a significant decrease in proliferation, whereas cells infected with the sh*Pbx3*-2 construct, which had the least degree of *Pbx3* knockdown, did not (Figure 5B).

Since pools of cells expressing a sh*Pbx3* may have variable levels of knockdown within individual clones, we isolated pure single cell clones infected with the sh*Pbx3*-3 lentivirus by limiting dilution. RQ-PCR demonstrated that expression of *Pbx3* was decreased by over 75% compared to uninfected 189MIG cells and NT-1 controls in two independent clones transduced with sh*Pbx3*-3 (sh*Pbx3*-3-2 and sh*Pbx3*-3-3) (Figure 5C). Figure 5D demonstrates that cells with decreased *Pbx3* expression proliferated at a significantly lower rate than uninfected and NT-1 controls. In addition, inhibition of *Pbx3* led to a dramatic decrease in the number of colony forming units (CFU) produced by the 189MIG cells in methylcellulose. The sh*Pbx3*-3-2 clone gave rise to no colonies and the sh*Pbx3*-3-3 gave rise to only 7 colonies, a 23-fold decrease compared to the NT1 control (Figure 5E).

To determine if the decrease in proliferation was due to differentiation of sh*Pbx3*-3 infected 189MIG cells, we analyzed the sh*Pbx3*-3 clones by flow cytometry for expression of differentiation markers including Mac1, Gr1, and Ter119, but saw no evidence of differentiation (data not shown). Analysis of PI stained cells did not indicate a G1 or G2 arrest, but did show a dramatic (10-fold) increase in sub-G1, apoptotic cells in sh*Pbx3*-3 subclones (Figure 5F). Taken together, these results suggest that continued *Pbx3* upregulation is important for the survival of cells that express the *NHD13* fusion, and therefore may be an important co-regulator of *NHD13*-mediated survival and transformation.

Discussion

Through a targeted gene resequencing approach we demonstrated that both *CA10* and *NHD13* mice have acquired Ras pathway mutations (Table 1), at a frequency similar to that seen in human AMLs [45]. Interestingly, we identified *Flt3* mutations as a frequent collaborating event in *CA10* but not *NHD13*-mediated leukemogenesis (Table 1) [28]. Although the most common *Flt3* mutations in the *CA10* mice were point mutations in the TKD, we documented for the first time a spontaneous *Flt3*-ITD in a mouse model of leukemia (Table 1). These *CA10* leukemias harboring *Flt3*-ITD mutations lost the WT *Flt3* allele in the leukemic clones (Figure 1 A–C), similar to human AML [31].

Gene expression profiling of *CA10* hematopoietic tissue and leukemias identified *Hoxa9* and *Meis1* as the two most consistent and significantly overexpressed genes in *CA10* transgenic mice, suggesting that an important downstream effect of *CA10* in the hematopoietic compartment is to promote dysregulation of *Hoxa9* and *Meis1*. This is consistent with GEPs obtained from leukemic patients harboring a MLL-rearrangement as well as *CA10* positive leukemias [34]. Utilizing GSEA, we show that the GEPs from *CA10* AMLs were similar to those from human *MLL*-rearranged leukemias (Figure 2B) [24, 25]. An additional comparison between the murine *CA10* leukemias and GEPs from patients with *CA10* T-ALL showed a significant overlap in genes that have been up-regulated (Supplemental Figure 1) [34, 35]. This data indicates that the *CA10* mouse model shares a similar biology to human leukema and that targeted therapies used to treat *CA10* might also be applicable to the treatment of *MLL*-rearranged leukemias.

MicroRNAs (miRNA) are small non-coding RNA molecules that regulate the stability and translation of mRNAs involved in wide range of biological processes including leukemogenesis [46]. mir196b is a miRNA embedded within the *Hoxa* locus in both humans

and mice, and is overexpressed in a subset of AML patients [47]. Although the upregulation of mir196b was initially noted in *MLL*-fusion leukemic samples [37, 47], subsequent studies demonstrated that samples from non *MLL*-fusion leukemias, including *CA10* and *SET-NUP214*, also showed overexpression of mir196b [38], suggesting that up-regulation of mir196b is associated with deregulation of the *Hoxa* locus by oncogenic fusion proteins. Therefore, in addition to the increase in *Hoxa* cluster gene expression, both the *CA10* and *NHD13* leukemias show upregulation of mir196b, underscoring the similarity of these leukemias to each other as well as *MLL*-fusion leukemias.

An important distinction between the *CA10* and *NHD13* murine leukemias was differential gene expression of TALE homeodomain family genes *Meis1* and *Pbx3*. *Meis1* was identified as a critical, rate limiting factor in *MLL*-induced leukemic transformation, although loss of both *Pbx2* and *Pbx3* could partially impair *MLL*-induced transformation [13]. Our findings suggest that, similar to *MLL*-fusions, up-regulation of *Meis1* as an important event in *CA10*-mediated transformation. However, *Meis1* expression was only modestly increased in the AML samples from *NHD13* mice and, in some cases, was decreased relative to WT BM (Supplemental Figure 1). Analysis of GEPs from *NHD13* thymus, BM, and LNBM revealed a consistent up-regulation of *Pbx3* (Figure 4B–D). In addition, knockdown of *Pbx3* expression in an *NHD13* cell line resulted in decreased proliferation, increased apoptosis, and a dramatic decrease in the ability to form colonies in methylcellulose (Figure 5) suggesting that loss of *Pbx3* is important to the maintenance and survival of cells overexpressing an *NHD13* fusion. This data is supported by a recent clinical report demonstrating that the co-expression of *Hoxa9* and *Pbx3* was an important predictor of poor outcome in a large subset of AML patients [48].

Through the use of several genetic approaches, we have identified genes and pathways that are similar or unique in leukemias triggered by expression of *CA10* or *NHD13*. Both fusion genes produce an AML that is associated with B-lineage features, and both overexpress *Hoxa* cluster genes similar to AMLs associated with *MLL* fusions. Although spontaneous *Flt3* mutations were not identified in the *NHD13*-induced AML [28], spontaneous *Flt3* mutations were common in the *CA10*-induced AMLs. We speculate that this may be due to the fact that the *CA10* mice overexpress *Flt3*, whereas NHD13 mice do not, as opposed to the possibility that the *NHD13* fusion can not collaborate with *Flt3* to transform cells. This hypothesis is supported by the observation that the *NHD13* fusion does in fact collaborate with a *Flt3* ITD mutation to generate AML in an experimental mouse model [49]. We have identified reciprocal expression of *Meis1* and *Pbx3* in the *CA10* and *NHD13* murine models and have also shown a functional role for *Pbx3* expression in *NHD13*-mediated transformation. Taken together, these murine models of AML provide tools to study pathways that cooperate with oncogenic fusions proteins and identify potential targets for AML treatment.

Supplementary Material

Refer to Web version on PubMed Central for supplementary material.

Acknowledgments

The authors thank Drs. Yang Jo Chung, Sheryl Gough, Masahiro Onoazawa, Hyunkyung Kim and Zhenhua Zhang for insightful discussions and Maria Jorge for expert technical assistance with the mouse colonies. This work was supported by the Intramural Research Program of the National Institutes of Health, National Cancer Institute. Gene expression analyses were performed using BRB-ArrayTools developed by Dr. Richard Simon and BRB-ArrayTools Development Team.

References

1. Rabbitts TH. Chromosomal translocations in human cancer. Nature. 1994; 372:143–149. [PubMed: 7969446]
2. Rowley JD. The role of chromosome translocations in leukemogenesis. Semin Hematol. 1999; 36:59–72. [PubMed: 10595755]
3. Ayton PM, Cleary ML. Molecular mechanisms of leukemogenesis mediated by MLL fusion proteins. Oncogene. 2001; 20:5695–5707. [PubMed: 11607819]
4. Gough SM, Slape CI, Aplan PD. NUP98 gene fusions and hematopoietic malignancies: common themes and new biologic insights. Blood. 2011; 118:6247–6257. [PubMed: 21948299]
5. Caudell D, Aplan PD. The role of CALM-AF10 gene fusion in acute leukemia. Leukemia : official journal of the Leukemia Society of America, Leukemia Research Fund, UK. 2008; 22:678–685.
6. Golub TR, Slonim DK, Tamayo P, et al. Molecular classification of cancer: class discovery and class prediction by gene expression monitoring. Science. 1999; 286:531–537. [PubMed: 10521349]
7. Palmqvist L, Pineault N, Wasslavik C, Humphries RK. Candidate genes for expansion and transformation of hematopoietic stem cells by NUP98-HOX fusion genes. PLoS One. 2007; 2:e768. [PubMed: 17712416]
8. Kawagoe H, Humphries RK, Blair A, Sutherland HJ, Hogge DE. Expression of HOX genes, HOX cofactors, and MLL in phenotypically and functionally defined subpopulations of leukemic and normal human hematopoietic cells. Leukemia : official journal of the Leukemia Society of America, Leukemia Research Fund, UK. 1999; 13:687–698.
9. Lawrence HJ, Christensen J, Fong S, et al. Loss of expression of the Hoxa-9 homeobox gene impairs the proliferation and repopulating ability of hematopoietic stem cells. Blood. 2005; 106:3988–3994. [PubMed: 16091451]
10. Afonja O, Smith JE Jr, Cheng DM, et al. MEIS1 and HOXA7 genes in human acute myeloid leukemia. Leuk Res. 2000; 24:849–855. [PubMed: 10996203]
11. Drabkin HA, Parsy C, Ferguson K, et al. Quantitative HOX expression in chromosomally defined subsets of acute myelogenous leukemia. Leukemia : official journal of the Leukemia Society of America, Leukemia Research Fund, UK. 2002; 16:186–195.
12. Iwasaki M, Kuwata T, Yamazaki Y, et al. Identification of cooperative genes for NUP98-HOXA9 in myeloid leukemogenesis using a mouse model. Blood. 2005; 105:784–793. [PubMed: 15454493]
13. Wong P, Iwasaki M, Somervaille TC, So CW, Cleary ML. Meis1 is an essential and rate-limiting regulator of MLL leukemia stem cell potential. Genes Dev. 2007; 21:2762–2774. [PubMed: 17942707]
14. Faber J, Krivtsov AV, Stubbs MC, et al. HOXA9 is required for survival in human MLL-rearranged acute leukemias. Blood. 2009; 113:2375–2385. [PubMed: 19056693]
15. Kroon E, Thorsteinsdottir U, Mayotte N, Nakamura T, Sauvageau G. NUP98-HOXA9 expression in hemopoietic stem cells induces chronic and acute myeloid leukemias in mice. EMBO J. 2001; 20:350–361. [PubMed: 11157742]
16. Caudell D, Zhang Z, Chung YJ, Aplan PD. Expression of a CALM-AF10 fusion gene leads to Hoxa cluster overexpression and acute leukemia in transgenic mice. Cancer Res. 2007; 67:8022–8031. [PubMed: 17804713]
17. Lin YW, Slape C, Zhang Z, Aplan PD. NUP98-HOXD13 transgenic mice develop a highly penetrant, severe myelodysplastic syndrome that progresses to acute leukemia. Blood. 2005; 106:287–295. [PubMed: 15755899]
18. Chung YJ, Choi CW, Slape C, Fry T, Aplan PD. Transplantation of a myelodysplastic syndrome by a long-term repopulating hematopoietic cell. Proc Natl Acad Sci U S A. 2008; 105:14088–14093. [PubMed: 18768819]
19. Kelly LM, Gilliland DG. Genetics of myeloid leukemias. Annu Rev Genomics Hum Genet. 2002; 3:179–198. [PubMed: 12194988]
20. Morse HC 3rd, Anver MR, Fredrickson TN, et al. Bethesda proposals for classification of lymphoid neoplasms in mice. Blood. 2002; 100:246–258. [PubMed: 12070034]

21. Kogan SC, Ward JM, Anver MR, et al. Bethesda proposals for classification of nonlymphoid hematopoietic neoplasms in mice. Blood. 2002; 100:238–245. [PubMed: 12070033]
22. Subramanian A, Tamayo P, Mootha VK, et al. Gene set enrichment analysis: a knowledge-based approach for interpreting genome-wide expression profiles. Proc Natl Acad Sci U S A. 2005; 102:15545–15550. [PubMed: 16199517]
23. Mootha VK, Lindgren CM, Eriksson KF, et al. PGC-1alpha-responsive genes involved in oxidative phosphorylation are coordinately downregulated in human diabetes. Nat Genet. 2003; 34:267–273. [PubMed: 12808457]
24. Mullighan CG, Kennedy A, Zhou X, et al. Pediatric acute myeloid leukemia with NPM1 mutations is characterized by a gene expression profile with dysregulated HOX gene expression distinct from MLL-rearranged leukemias. Leukemia : official journal of the Leukemia Society of America, Leukemia Research Fund, UK. 2007; 21:2000–2009.
25. Ross ME, Mahfouz R, Onciu M, et al. Gene expression profiling of pediatric acute myelogenous leukemia. Blood. 2004; 104:3679–3687. [PubMed: 15226186]
26. Slape C, Chung YJ, Soloway PD, Tessarollo L, Aplan PD. Mouse embryonic stem cells that express a NUP98-HOXD13 fusion protein are impaired in their ability to differentiate and can be complemented by BCR-ABL. Leukemia : official journal of the Leukemia Society of America, Leukemia Research Fund, UK. 2007; 21:1239–1248.
27. Matozaki T, Murata Y, Saito Y, Okazawa H, Ohnishi H. Protein tyrosine phosphatase SHP-2: a proto-oncogene product that promotes Ras activation. Cancer Sci. 2009; 100:1786–1793. [PubMed: 19622105]
28. Slape C, Liu LY, Beachy S, Aplan PD. Leukemic transformation in mice expressing a NUP98-HOXD13 transgene is accompanied by spontaneous mutations in Nras, Kras, and Cbl. Blood. 2008; 112:2017–2019. [PubMed: 18566322]
29. Small D. FLT3 mutations: biology and treatment. Hematology Am Soc Hematol Educ Program. 2006:178–184. [PubMed: 17124058]
30. Bacher U, Haferlach C, Kern W, Haferlach T, Schnittger S. Prognostic relevance of FLT3-TKD mutations in AML: the combination matters--an analysis of 3082 patients. Blood. 2008; 111:2527–2537. [PubMed: 17965322]
31. Thiede C, Steudel C, Mohr B, et al. Analysis of FLT3-activating mutations in 979 patients with acute myelogenous leukemia: association with FAB subtypes and identification of subgroups with poor prognosis. Blood. 2002; 99:4326–4335. [PubMed: 12036858]
32. Dik WA, Brahim W, Braun C, et al. CALM-AF10+ T-ALL expression profiles are characterized by overexpression of HOXA and BMI1 oncogenes. Leukemia : official journal of the Leukemia Society of America, Leukemia Research Fund, UK. 2005; 19:1948–1957.
33. Asnafi V, Radford-Weiss I, Dastugue N, et al. CALM-AF10 is a common fusion transcript in T-ALL and is specific to the TCRgammadelta lineage. Blood. 2003; 102:1000–1006. [PubMed: 12676784]
34. Grossmann V, Bacher U, Kohlmann A, et al. EZH2 mutations and their association with PICALM-MLLT10 positive acute leukaemia. British journal of haematology. 2012; 157:387–390. [PubMed: 22235851]
35. Mulaw MA, Krause AJ, Deshpande AJ, et al. CALM/AF10-positive leukemias show upregulation of genes involved in chromatin assembly and DNA repair processes and of genes adjacent to the breakpoint at 10p12. Leukemia : official journal of the Leukemia Society of America, Leukemia Research Fund, UK. 2012; 26:1012–1019.
36. Choi CW, Chung YJ, Slape C, Aplan PD. A NUP98-HOXD13 fusion gene impairs differentiation of B and T lymphocytes and leads to expansion of thymocytes with partial TCRB gene rearrangement. J Immunol. 2009; 183:6227–6235. [PubMed: 19841179]
37. Popovic R, Riesbeck LE, Velu CS, et al. Regulation of mir-196b by MLL and its overexpression by MLL fusions contributes to immortalization. Blood. 2009; 113:3314–3322. [PubMed: 19188669]
38. Schotte D, Lange-Turenhout EA, Stumpel DJ, et al. Expression of miR-196b is not exclusively MLL-driven but is especially linked to activation of HOXA genes in pediatric acute lymphoblastic leukemia. Haematologica. 2010; 95:1675–1682. [PubMed: 20494936]

39. Wang Y, Li Z, He C, et al. MicroRNAs expression signatures are associated with lineage and survival in acute leukemias. Blood Cells Mol Dis. 2010; 44:191–197. [PubMed: 20110180]
40. Cammarata G, Augugliaro L, Salemi D, et al. Differential expression of specific microRNA and their targets in acute myeloid leukemia. Am J Hematol. 2010; 85:331–339. [PubMed: 20425795]
41. Moens CB, Selleri L. Hox cofactors in vertebrate development. Dev Biol. 2006; 291:193–206. [PubMed: 16515781]
42. Roche J, Zeng C, Baron A, et al. Hox expression in AML identifies a distinct subset of patients with intermediate cytogenetics. Leukemia : official journal of the Leukemia Society of America, Leukemia Research Fund, UK. 2004; 18:1059–1063.
43. Wang GG, Pasillas MP, Kamps MP. Meis1 programs transcription of FLT3 and cancer stem cell character, using a mechanism that requires interaction with Pbx and a novel function of the Meis1 C-terminus. Blood. 2005; 106:254–264. [PubMed: 15755900]
44. Palmqvist L, Argiropoulos B, Pineault N, et al. The Flt3 receptor tyrosine kinase collaborates with NUP98-HOX fusions in acute myeloid leukemia. Blood. 2006; 108:1030–1036. [PubMed: 16861351]
45. Bowen DT, Frew ME, Hills R, et al. RAS mutation in acute myeloid leukemia is associated with distinct cytogenetic subgroups but does not influence outcome in patients younger than 60 years. Blood. 2005; 106:2113–2119. [PubMed: 15951308]
46. Marcucci G, Mrozek K, Radmacher MD, Garzon R, Bloomfield CD. The prognostic and functional role of microRNAs in acute myeloid leukemia. Blood. 2011; 117:1121–1129. [PubMed: 21045193]
47. Schotte D, Chau JC, Sylvester G, et al. Identification of new microRNA genes and aberrant microRNA profiles in childhood acute lymphoblastic leukemia. Leukemia : official journal of the Leukemia Society of America, Leukemia Research Fund, UK. 2009; 23:313–322.
48. Li Z, Huang H, Li Y, et al. Up-regulation of a HOXA-PBX3 homeobox-gene signature following down-regulation of miR-181 is associated with adverse prognosis in patients with cytogenetically abnormal AML. Blood. 2012; 119:2314–2324. [PubMed: 22251480]
49. Greenblatt S, Li L, Slape C, et al. Knock-in of a FLT3/ITD mutation cooperates with a NUP98-HOXD13 fusion to generate acute myeloid leukemia in a mouse model. Blood. 2012; 119:2883–2894. [PubMed: 22323452]

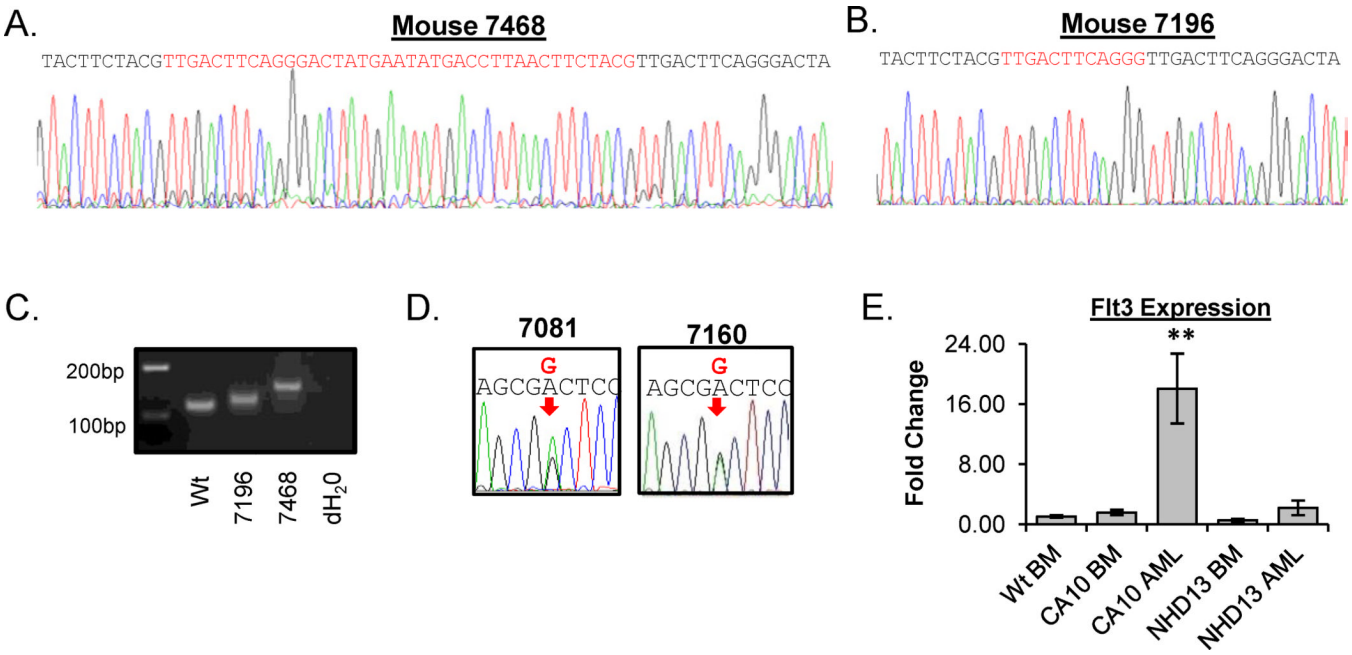

Figure 1. *CALM-AF10* AMLs acquire *Flt3* mutations

(A) and **(B)** Sequence tracings from *CA10* AML samples 7468 and 7196 harboring 39 bp and 12 bp insertions in *Flt3* exon 19. Red sequences represent the inserted sequences and the black sequences represent the WT sequences. **(C)** PCR analysis of genomic DNA from WT and *CA10* infiltrated spleens using primers that flanked the ITD. Note the absence of the WT allele in samples 7196 and 7468. **(D)** Sequence tracings from two *CA10* mice with a *Flt3*-TKD mutation. Note the presence of two peaks (mutant and WT) for the TKD mutations (indicated with a red arrow). **(E)** RQ-PCR analysis of *Flt3* expression in WT BM (n=4), *CA10* clinically healthy BM (n=3), *CA10* AML (n=5), *NHD13* clinically healthy BM (n=4) and *NHD13* AML (n=16). 18S ribosomal RNA was used as an internal control and samples were normalized to WT BM.

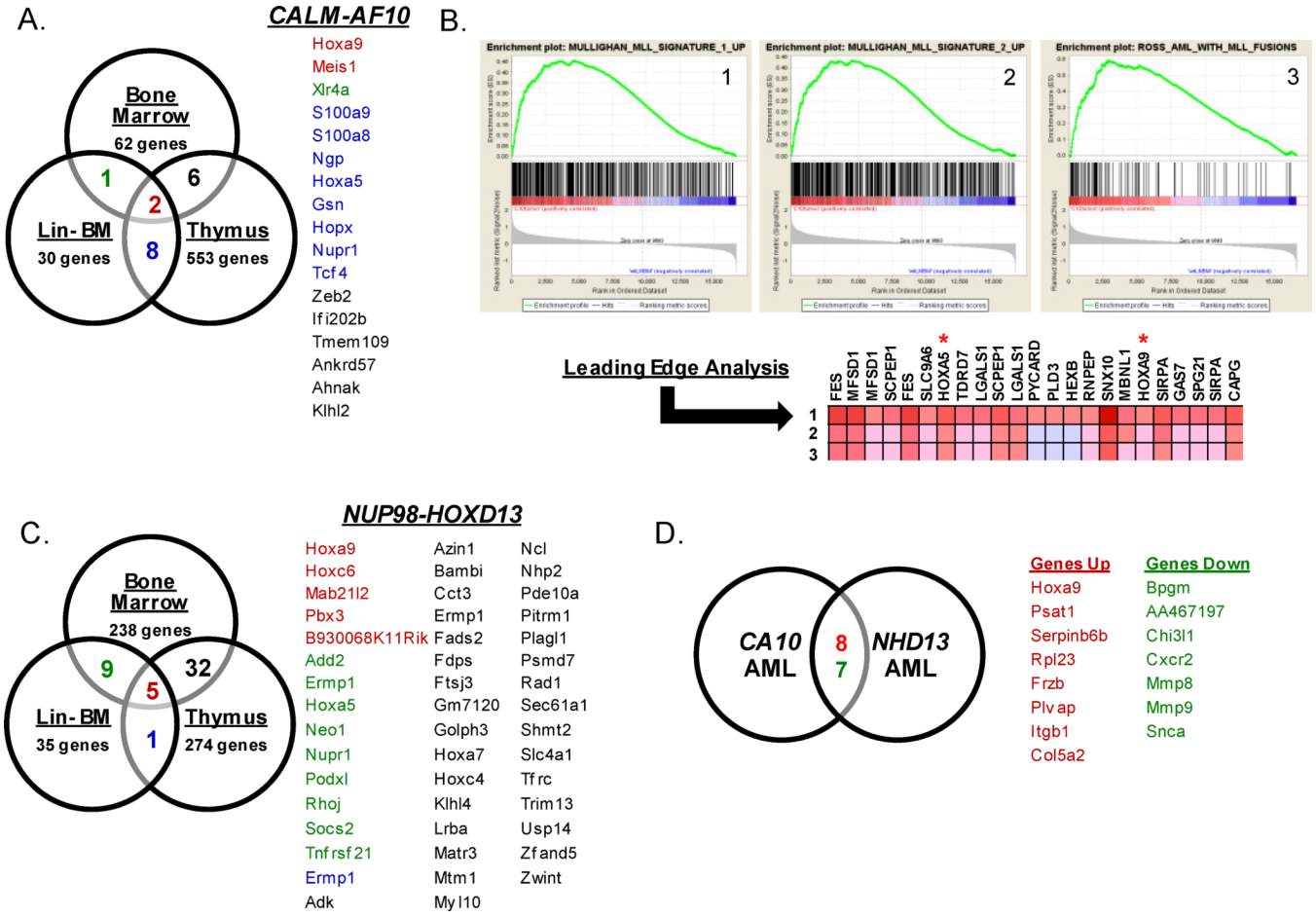

Figure 2. Analysis of gene expression profiles from *CA10* and *NHD13* mice

(A) Venn diagram of *CA10* BM, thymus and LNBM. List of genes common to tissues are colored according to the tissues where they overlap. Genes labeled in red correspond to genes common in all *CA10* tissues analyzed. **(B)** Gene Set Enrichment Analysis (GSEA) Leading Edge Analysis of *CA10* AML versus WT LNBM compared to AML gene signatures [24, 25]. **(C)** Venn diagram of *NHD13* BM, thymus and LNBM. **(D)** Venn diagram of gene expression of profiles from *CA10* and *NHD13* AMLs compared to WT LNBM. Genes labeled in red correspond to genes upregulated in both gene sets and genes labeled in green correspond to genes down-regulated in both gene sets.

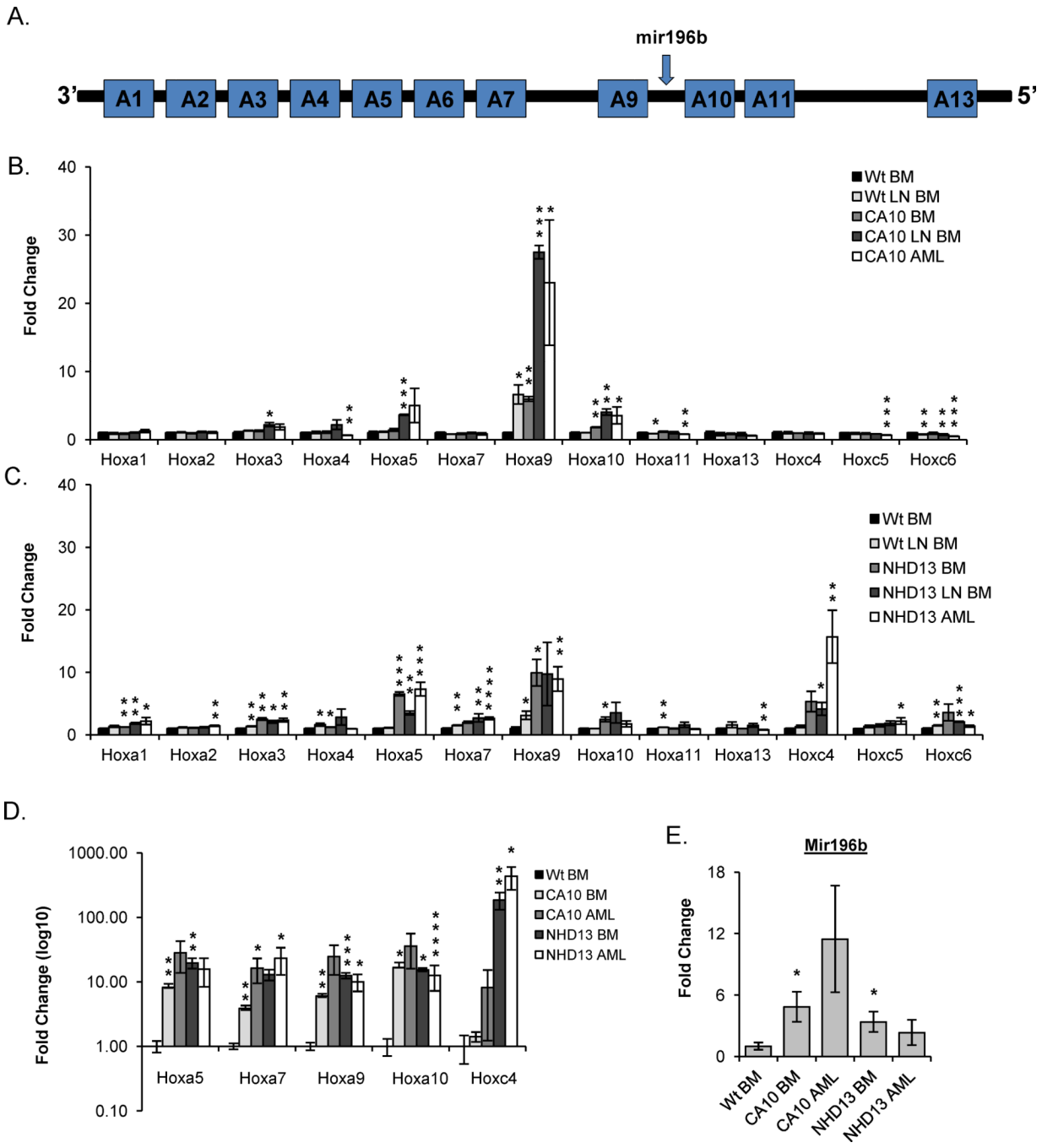

Figure 3. *CA10* and *NHD13* mice up-regulate *Hoxa* cluster genes

(A) Schematic of *Hoxa* locus including the microRNA mir196b. **(B)** *Hoxa* and *Hoxc* cluster gene expression data from expression arrays for WT LNBM (n=3), *CA10* BM (n=3), *CA10* LNBM (n=3) and *CA10* AMLs (n=6) normalized to WT BM (n=3). **(C)** *Hoxa* and *Hoxc* cluster gene expression data from expression arrays for WT LNBM (n=3), *NHD13* BM (n=3), *NHD13* LNBM (n=3) and *NHD13* AMLs (n=6) normalized to WT BM (n=3). **(D)** RQ-PCR confirmation of the up-regulation of *Hoxa5*, *Hoxa7*, *Hoxa9*, *Hoxa10* and *Hoxc4* in *CA10* BM (n=3), *CA10* AML (n=5), *NHD13* BM (n=5), and *NHD13* AMLs (n=5) normalized to WT BM (n=4). **(E)** RQ-PCR analysis of mir196b expression in *CA10* BM

(n=3), *CA10* AML (n=6), *NHD13* BM (n=3) and *NHD13* AML (n=6) normalized to WT BM (n=3). * , **, and *** indicate p<0.05, 0.01, and 0.001 respectively.

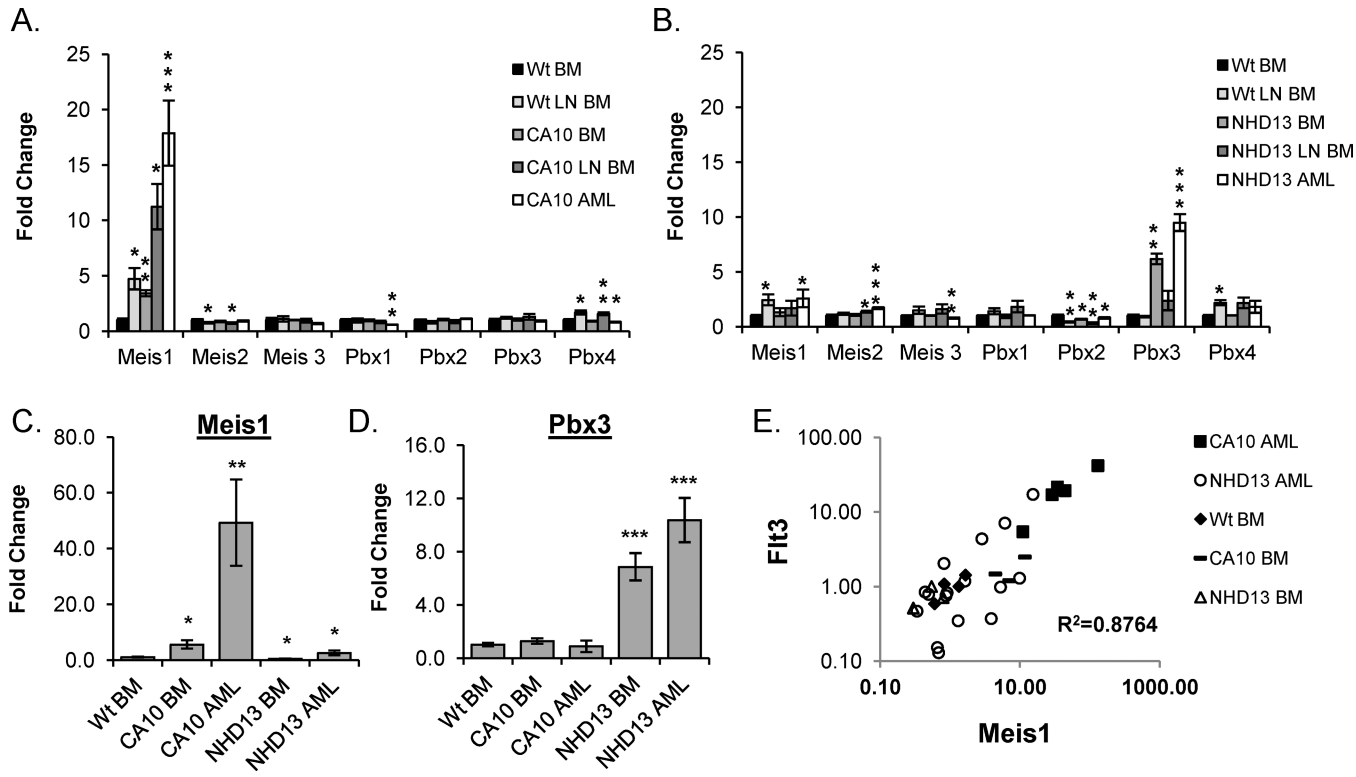

Figure 4. Differential expression of TALE homeodomain family genes in *CA10* and *NHD13* tissues

(A) Expression of TALE homeodomain genes from expression arrays for WT LNBM (n=3), *CA10* BM (n=3), *CA10* LNBM (n=3) and *CA10* AML (n=6), normalized to WT BM (n=3). **(B)** Expression of the TALE homeodomain genes from expression arrays for WT LNBM (n=3), *NHD13* BM (n=3), *NHD13* LNBM (n=3) and *NHD13* AML (n=6), normalized to WT BM (n=3). **(C and D)** Expression of *Meis1* and *Pbx3* measured by RQ-PCR in *CA10* BM (n=4), *CA10* AML (n=7), *NHD13* BM (n=5), and *NHD13* AML (n=16) normalized to WT BM (n=4). **(E)** *Meis1* and *Flt3* expression values for *CA10* BM (n=3), *CA10* AML (n=5), *NHD13* BM (n=4) and *NHD13* AML (n=16) were normalized to WT BM (n=4), plotted, and the correlation coefficient calculated. * , **, and *** indicate $p<0.05$, 0.01, and 0.001 respectively.

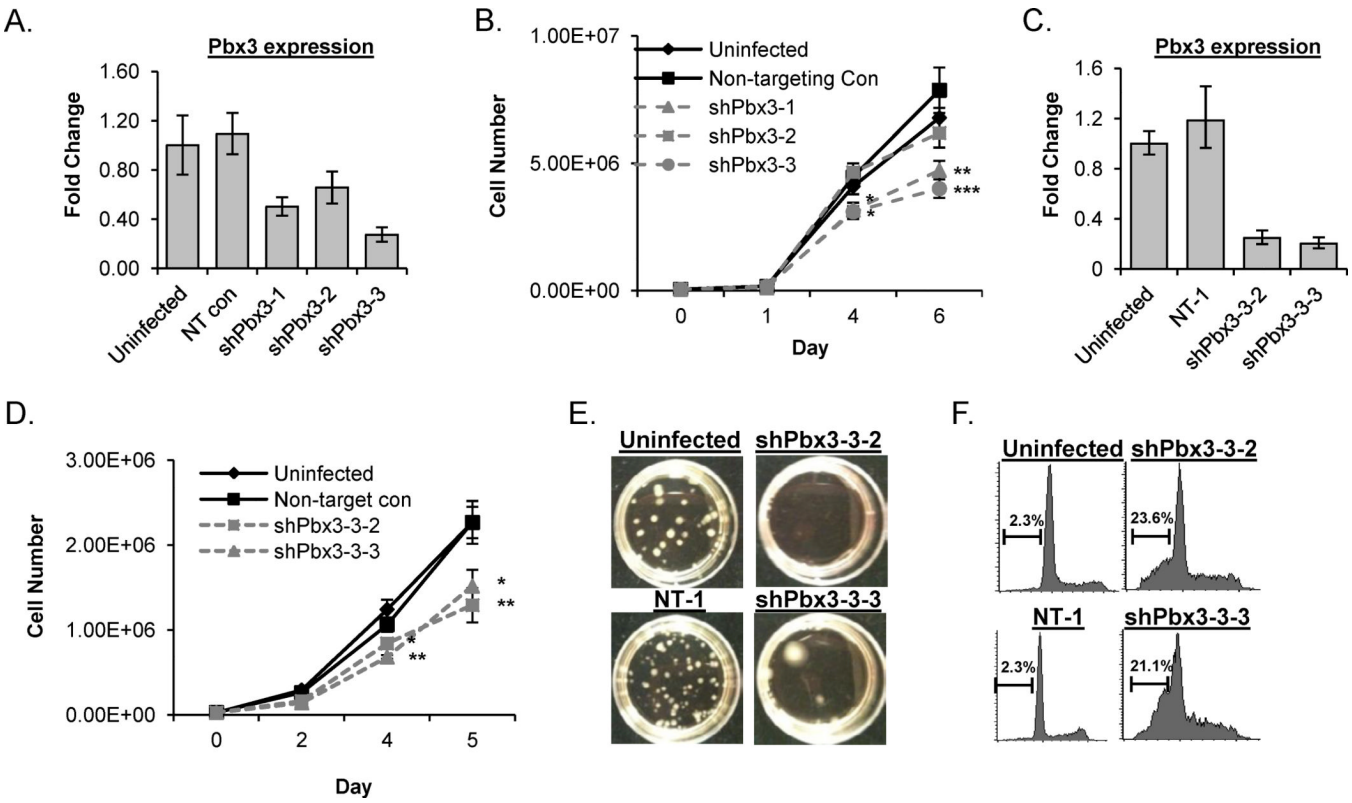

Figure 5. Knockdown of *Pbx3* inhibits proliferation and promotes apoptosis in a *NHD13* cell line

(A) RQ-PCR analysis for *Pbx3* expression from pools of 189MIG cells infected with shRNA against a non-targeting (NT) control or *Pbx3* (sh*Pbx3*-1, sh*Pbx3*-2, and sh*Pbx3*-3) compared to uninfected 189 MIG cells. **(B)** Proliferation curves of pooled clones from uninfected, NT control, sh*Pbx3*-1, sh*Pbx3*-2, and sh*Pbx3*-3 infected cells. **(C)** RQ-PCR analysis of *Pbx3* expression from single cell clones of 189MIG cells infected with the NT control (NT-1) and two clones infected with sh*Pbx3*-3 (designated sh*Pbx3*-3-2 and sh*Pbx3*-3-3), compared to uninfected 189MIG cells. **(D)** Proliferation curves from single cell clones from NT-1 and sh*Pbx3*-3-2 and sh*Pbx3*-3-3 compared to uninfected 189MIG cells. **(E)** Analysis of uninfected, NT-1, sh*Pbx3*-3-2 and sh*Pbx3*-3-3 in methylcellulose CFU assay **(F)** Measurement of DNA content from uninfected 189MIG, NT-1 shRNA control, sh*Pbx3*-3-2 and sh*Pbx3*-3-3 at day 5 in liquid culture. Apoptotic events are those with less than 2N DNA. * , **, and *** indicate $p<0.05$, 0.01, and 0.001 respectively.

Table 1

Targeted gene resequencing of *CALM-AF10* leukemic mice

Mouse	IgH rgmt	*Nras*	*Kras*	*Ptpn11*	*Flt3*
2953	yes	GL	codon 12 GGT>GCT (G>A)	GL	codon 822 GTC>GCC (V>A)
7026	no	GL	GL	GL	GL
7081	no	GL	GL	GL	codon 841 GAC>GGC (D>G)
7088	no	codon 12 GGT>GAT (G>D)	GL	GL	codon 841 GAC>GGC (D>G)
7092	yes	GL	GL	codon 76 GAA>AAA (E>K)	GL
7095	yes	GL	GL	GL	GL
7160	yes	GL	GL	GL	codon 841 GAC>GGC (D>G)
7196	ND	GL	GL	GL	12 bp duplication
7214	yes	GL	GL	GL	GL
7223	no	GL	GL	GL	GL
7249	ND	GL	GL	GL	GL
7280	ND	GL	GL	GL	GL
7339	ND	GL	GL	GL	GL
7408	ND	GL	GL	GL	GL
7412	ND	GL	GL	GL	GL
7415	ND	GL	GL	GL	GL
7438	ND	GL	GL	GL	GL
7468	yes	GL	GL	GL	39 bp duplication
7520	ND	GL	GL	GL	GL
7541	ND	codon 61 CAA>CAT (Q>H)	GL	GL	GL
9001	yes	GL	GL	GL	GL
9010	yes	codon 13 GGT>GAT (G>D)	GL	GL	GL
9014	no	GL	GL	GL	GL
9043	yes	GL	GL	GL	codon 837 in frame deletion (D)
9068	yes	GL	GL	GL	codon 841 GAC>GGC (D>G)
9120	ND	GL	GL	GL	GL
9139	yes	GL	codon 61 CAA>CGA (Q>R)	GL	GL

ND- Not done